New Insights Concerning Intrinsic Joint Elasticity for Safety

Sami Haddadin, Alin Albu-Schäffer, Oliver Eiberger, and Gerd Hirzinger

***Abstract*— In this paper we present various new insights on the effect intrinsic joint elasticity has on safety in pHRI. We address the fact that the intrinsic safety of elastic mechanisms has been discussed rather one sided in favor of this new designs and intend to give a more differentiated view on the problem. An important result is that intrinsic joint elasticity does not reduce the Head Injury Criterion or impact forces compared to conventional actuation with some considerable elastic behavior in the joint, if considering full scale robots. We also elaborate conditions under which intrinsically compliant actuation is potentially more dangerous than rigid one. Furthermore, we present collision detection and reaction schemes for such mechanisms and verify their effectiveness experimentally.**

I. Introduction

Recently, there is increasing interest in domestic and industrial service robots that allow physical interaction [1], [2], [3]. The goal of robots and humans coexisting in the same physical domain poses various fundamental problems for the entire robotic design. The most stringent requirement is to prevent human injury by any means. Unlike their classical counterparts, robots that interact with humans need to take into account for the hardware design, control, and planning that the environment is partially *unknown*. Therefore, the robot must react compliantly to unexpected contact with the environment or humans. In this sense, there has been strong interest in realizing intrinsic safety by means of mechanical design and thus decouple control schemes to a certain extent from the burden of realizing human-friendly behavior [4], [5]. The concept of variable stiffness actuation (VSA)[1] seems to be a promising solution in this context [6], [4], [7], [8], [9], [10]. One of the main objectives to introduce variable compliance has been to increase safety for the human. At the same time the maximization of task performance, joint protection against external shocks, and the task dependent compliance adaptation are aimed at [6], [11], [12], [13]. In general, future robotic systems are supposed to execute tasks with similar speed and dexterity to humans. However, the human peak performance, e.g. in terms of maximum joint velocity (take e.g. the shoulder rotation speed of $6.900 - 9800\ ^\circ/s$ during a baseball pitch of a professional pitcher [14]) is currently not realizable if the torque range and the weight of the joint should also match with human properties. Therefore, another argument in favor of intrinsic joint compliance is its capability to store and release elastic energy. This can e.g. be used for energy efficient cyclic motions or for increasing the top speed of the link beyond maximum motor velocity [15], [10]. Especially the latter capability brings up entirely new aspects in terms of safety. In this paper we discuss the related effects and provide an analysis of the intrinsic collision behavior of VIA joints during robot-human impacts. We extend existing safety investigations, as e.g. carried out in [4], [16], [17], and provide significant aspects to be considered in the ongoing discussion of elastic actuation. Furthermore, we elaborate and evaluate collision detection and reaction schemes for intrinsically compliant joints. In this paper we use the DLR QA-Joint [13], which is a prototype for the anthropomorphic DLR Hand-Arm system [18], as our testbed to support our results.

The paper is organized as follows. Section II elaborates the basic conditions during robot-human impacts with intrinsically compliant joints. Section III presents the results from different robot-human impact simulations. Furthermore, we give some general analysis on how the potential velocity increase with elastic actuators affects their safety characteristics. In Section IV we introduce collision detection methods suited for VIA and analyze their performance. Finally, Sec. V concludes the work.

II. Compliance for safety

In this section we discuss some typical properties during blunt human-robot impacts with VIA joints. Generally, one can identify two immediate sources of possible human injury during direct contact with a robot, namely sharp or blunt contacts [19]. Even though soft-tissue injury has recently received increasing attention in the robotics community [20], [21], [22] we want to focus on blunt human-robot impacts in this paper. In general, the use of intrinsic joint compliance was mostly motivated by the desired decoupling of motor and link inertia during unexpected collisions. This effect reduces the collision danger by alleviating the impacting robot inertia. In [4] it is e.g. shown that the Head Injury Criterion (HIC), which is a biomechanical injury criterion associated with head acceleration, could be reduced by introducing elasticity in the joint. The HIC is defined as

$$\mathrm{HIC}_{36} = \max_{\Delta t} \left\{ \Delta t \left(\frac{1}{\Delta t} \int_{t_1}^{t_2} ||\ddot{\mathbf{x}}_H||_2 \mathrm{d}t \right)^{\left(\frac{5}{2}\right)} \right\} \leq 1000 \quad (1)$$
$$\Delta t = t_2 - t_1 \leq \Delta t_{\max} = 36 \text{ ms},$$

where $||\ddot{\mathbf{x}}_H||$ is the resulting acceleration of the human head and has to be measured in $\mathrm{g} = 9.81$ m/s^2.

As pointed out in [4] a joint with quite low reflected link inertia $M_x = 0.1$ kg is able to significantly reduce the impact characteristics (by means of HIC) if a contact stiffness of $K_H = 5$ kN/m is assumed. Basically, the following assumptions were made:

$$\text{stiff}: \quad B_x >> M_x \quad M_x << M_H \quad K_{J,x} >> K_H \quad (2)$$
$$\text{compliant}: \quad B_x >> M_x \quad M_x << M_H \quad K_{J,x} << K_H, \quad (3)$$

S. Haddadin, A. Albu-Schäffer, E. Eiberger, and Gerd Hirzinger are with Institute of Robotics and Mechatronics, DLR - German Aerospace Center, Wessling, Germany sami.haddadin, oliver.eiberger, alin.albu-schaeffer@dlr.de

[1]Or its generalization of variable impedance actuation (VIA).

where $M_x, M_H, K_H \in \mathbb{R}^+$ are the reflected link inertia, head mass, and head stiffness. $B_x, K_{J,x} \in \mathbb{R}^+$ are the reflected motor inertia and joint stiffness. Similarly to the work in [5] it was derived that a decrease in joint stiffness can drastically reduce the impact characteristics and thus is a powerful countermeasure against large contact forces under the given assumptions. [17] analyzed the case of a 2DoF planar intrinsically compliant robot that already slightly touches a rigid wall with its second link. The authors deduced that the compliant mechanism can limit the maximum static force/torque effectively if the motor torque is slowly increased. The corresponding conditions are

$$\text{stiff}: \quad M_x \approx 0 \quad B_x << M_H \quad K_{J,x} < K_H \quad (4)$$

$$\text{compliant}: \quad M_x \approx 0 \quad B_x << M_H \quad K_{J,x} << K_H \quad (5)$$

In the cited work fundamental insights concerning the influence of joint elasticity on safety were given for different impact conditions. It is of course unquestionable that joint elasticity decouples the motor from the link. However, as was indicated in [12], we observed that a reduction in joint stiffness cannot attenuate the impact characteristics during very rigid and fast crash-test dummy impacts with the DLR Lightweight Robot III (LWR-III). This was proven by measuring the decoupling of motor and link inertia via the integrated joint torque sensor and the additionally recorded external contact force. This observation was quite surprising to us and shows that already the compliance of the built in Harmonic Drive and of the joint torque sensor is sufficient to decouple motor from link. This makes it entirely unnecessary to further reduce joint stiffness for the given robot. There are two main aspects, which have to be considered to fully understand this result. On the one hand, the contact stiffness of the used crash-test dummy is significantly larger ($K_H \approx 10^6$ N/m) than the reflected elasticity of the LWR-III ($K_{J,x} \approx 10^5$ N/m). Furthermore, the reflected motor and link inertia of the LWR-III are $B_x \approx 13$ kg and $M_x \approx 4$ kg for the experiment. This means that the reflected link inertia is in the order of magnitude of the head mass. The corresponding mass and stiffness relations are therefore:

$$B_x > M_x \quad M_x \approx M_H \quad K_{J,x} << K_H \quad (6)$$

This is obviously a different siuation from (2) and (4). This aspect is, however, not unique for the LWR-III but of more general character. Consider the most simple two-link manipulator (q_1, q_2), having only point masses m_1, m_2 at its distal end of each link. The associated Operational space mass matrix in body coordinates may be written as

$$M_x(\mathbf{q}) = \begin{bmatrix} m_2 + \frac{m1}{\sin^2(q_2)} & 0 \\ 0 & m_2 \end{bmatrix} \quad (7)$$

The $x-$axis is pointing along the main axis of the second link. When considering the stretched out configuration and hitting the head in $y-$direction, the reflected inertia in this direction is simply m_2. Now let us assume that the arm has more or less human like inertia properties with link weights $m_{1,2} \approx 2$ kg (Please note this is a very ambitious target weight for a full robot with similar torque capacities compared to the human.). There is to the best of our knowledge no manipulator yet available that realizes such desired properties. However, this would mean that the impact mass involved in the robot-human impact is $M_x = 2$ kg, i.e. $M_x \approx M_H$ ($M_H \approx 4$ kg). Since the contact properties of human facial bones are also in similar range as the dummy head condition (6) can be assumed to be very realistic. This is due to the fact that such a hypothetical light arm would have at least similar flexibility in the joints as the LWR-III.

To sum up, for a full-scale robot the desired decoupling effect between motor and link inertia during rigid head impacts takes already place for quite high joint stiffness. This is mainly due to the very high contact stiffness of the human head and implies that elastic actuation does not improve the effect considerably.

III. Blunt impact dynamics

In this section we present simulation results of impacting the QA-Joint (1DoF) at different impact speeds and stiffness presets with the human head and abdomen. Furthermore, we derive some theoretical insight into the intrinsic properties of human-robot collisions with VIA joints. For the simulations we assume following model

$$B\ddot{\theta} = \tau_m - \tau_J(\varphi, \sigma) \quad (8)$$

$$M\ddot{q} = \tau_J(\varphi, \sigma) - \tau_F - \tau_g - \tau_{\text{ext}}, \quad (9)$$

where $B, M \in \mathbb{R}^+$ are the motor and link side inertia. $\theta, q \in \mathbb{R}$ the motor and link side position, $\varphi = \theta - q$ the elastic deflection, and $\tau_m, \tau_J(\varphi, \sigma), \tau_F, \tau_g, \tau_{\text{ext}} \in \mathbb{R}$ the motor, elastic, friction, gravity, and external torque. $\sigma \in \mathbb{R}$ is the stiffness adjuster position. For sake of clarity we assume $\tau_F = \tau_g = 0$.

For the DLR QA-Joint the elastic joint torque is defined as

$$\tau_J = 40(e^{15((\theta-q)-\sigma)} - e^{15((\theta-q)-\sigma)}). \quad (10)$$

For details on the human models used in the impact simulations to generate τ_{ext}, as well as the joint design please refer to [23], [15] and [13]. Furthermore, we use the state feedback controller introduced in [24] for achieving good tracking performance of the QA-Joint. For all collision simulations we command a smooth trapezoidal velocity profile to hit the human body part at constant link velocity and without significant elastic deflection. Furthermore, we assume the motor torque to be bounded.

A. Head Injury Criterion

Figure 1 (left) shows the Head Injury Criterion for three different stiffness presets and various impact velocities. The tip impact velocity ranges up to 1.3 m/s and the stiffness preset is set to very low, medium, and high stiffness adjustment ($\sigma \in \{1 \quad 6 \quad 11\}$ deg). As already observed for rigid robots or for robots with moderate joint compliance as the LWR-III [25], [12], [26], Fig. 1 clearly supports the statement of high impact velocity dependency of HIC also for a VIA joint. However, at the same time it becomes clear that an impact at such speeds with the QA-Joint is definitely not harmful by means of HIC. The HIC reaches maximum values of ≈ 10, representing a practically negligible injury probability [12]. Furthermore, it cannot be confirmed that HIC significantly depends on joint stiffness. The curve is very similar to the

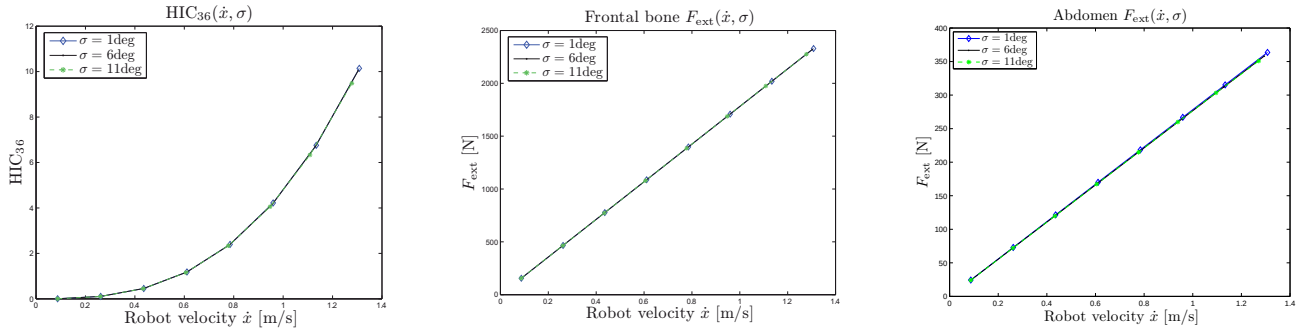

Fig. 1. Head Injury Criterion for different joint velocities and stiffness values (left). Frontal impact force for different joint velocities and stiffness values (middle). Abdominal impact force for different joint velocities and stiffness values (right).

one for a quite stiff joint (e.g. non negligible joint elasticity due to Harmonic Drive and joint torque sensor). In other words, the joint inertias (motor and link) are decoupled for all stiffness presets already. Therefore, high stiffness of an intrinsically compliant joint is already low enough to decouple motor and link inertia during a rigid impact compared to "industrial" robot rigidity. This seems to be a very surprising result and significantly changes the knowledge about the role intrinsic joint compliance plays for safety. Basically, there is no need to demand more joint compliance than e.g. the intrinsic one of the LWR-III. This observation holds already for quite low reflected link inertias. We may say that for practically relevant inertias, joint elasticity in the range that is characteristic for intrinsically compliant joints does not add additional safety for head impacts.

The main reason for this effect is that the head stiffness is very high and compared to rigid joints of the LWR-III already two orders of magnitude larger (see Sec. II).

B. Frontal impact force

Figure 1 (middle) shows the impact force for the frontal bone, pointing out the linear relationship between peak force and impact velocity as described in [23]. This simulation also confirms that decoupling of motor from link inertia is present during all impacts. Please note that even though the contact forces get quite large, they are still far below the corresponding fracture threshold value of 4 kN for the frontal bone. This leads to the conclusion that frontal fractures are very unlikely to occur.

C. Abdominal impact force

Figure 1 (right) shows the impact force for the abdomen, having similar behavior as the frontal impact force. For this simulation the mass of the human is considerably higher and the stiffness is lower by two orders of magnitude compared to the frontal skull area. However, also for this simulation the decoupling already applies due to the still lower joint stiffness compared to the human abdomen. Again, the occurring impact forces are significantly smaller than any critical value. Therefore, one can conclude that such an impact is not causing any harm to the human abdominal area by means of the force criterion. This states that a contact force of 2.5 kN must not be exceeded.

D. Maximum HIC for compliant joints

Intrinsic joint compliance is often considered to be the key to intrinsic safety. As is argued in this part of the paper, this statement needs some relevant extension, since there is clear evidence that under certain circumstances even the contrary may be concluded.

Let us consider the effect energy storage has on head injury again by means of HIC. We treat an open-loop system with respect to the link side position q. Furthermore, we assume the already mentioned decoupling effect. According to [27] HIC can be expressed as

$$\text{HIC} = 2\left(\frac{M_x}{(M_x+M_H)g}\right)^{\frac{5}{2}}\alpha^{-\frac{3}{2}}(\sin\alpha)^{-\frac{5}{2}}\left(\frac{M_x+M_H}{M_xM_H}\right)^{\frac{3}{4}}K_H^{\frac{3}{4}}||\dot{\mathbf{x}}_0||^{\frac{5}{2}} \tag{11}$$

when assuming a simple mass-spring model of the human head. $\dot{\mathbf{x}}_0$ is the Cartesian robot impact velocity. The constant α is

$$\alpha = \min(\alpha^*, \omega\Delta t_{\max}/2), \tag{12}$$

where α^* is the solution of

$$3\sin\alpha - 5\alpha\cos\alpha = 0 \tag{13}$$

in $[0, \pi/2]$. ω is defined as

$$\omega := \sqrt{\frac{(M_x+M_H)K_H}{M_xM_H}}. \tag{14}$$

In [12] we used a more sophisticated nonlinear model for analysis which does not allow such a solution of HIC. However, the simple mass-spring model is sufficient for extracting some conclusions in the following. As one can see from (1), impact velocity affects HIC more than quadratically. When considering the infinite mass robot $M_x \to \infty$ in (11) it becomes clear that HIC saturates

$$\text{HIC} = 2g^{-\frac{5}{2}}\alpha^{-\frac{3}{2}}(\sin\alpha)^{-\frac{5}{2}}M_H^{-\frac{3}{4}}K_H^{\frac{3}{4}}||\dot{\mathbf{x}}_0||^{\frac{5}{2}}. \tag{15}$$

Up to now this evaluation is for rigid robots with reflected inertia M (consisting for very rigid industrial robots of the motor and link inertia) as well as for decoupled compliant robots with link side reflected inertia M_x. As e.g. described in [15] it is possible to store a considerable amount of energy in the elastic mechanism of a VIA joint and use it for significant speedup of the link. Very high velocity

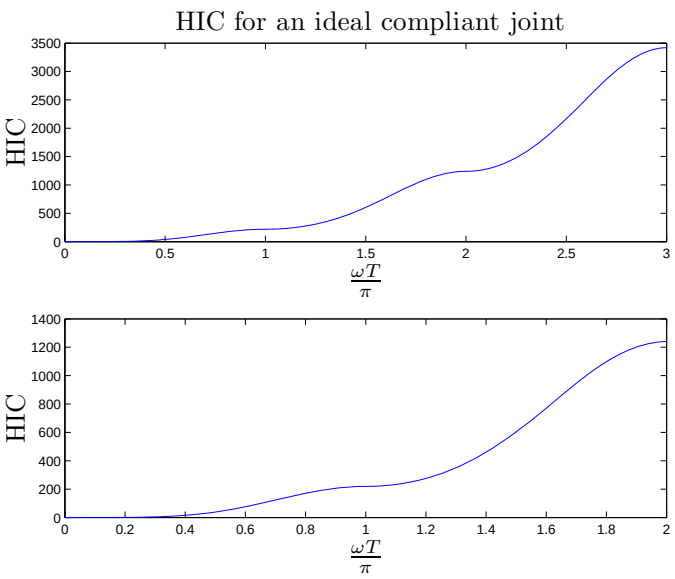

Fig. 2. Ideal HIC values for a compliant joint with constant joint stiffness $K = 10^6$ N/m and maximum motor velocity $\dot{\theta}_{\max} = 220$ deg/sec. The upper plot shows HIC for a windup time of up to $\frac{\omega T}{\pi} = 3$ and the lower one for up to $\frac{\omega T}{\pi} = 1.5$.

could be achieved if one is able to apply bang-bang control and no elastic joint limits would be present. However, some oscillation cycles are still easily possible even if real-world constraints as e.g. maximum deflection are considered. Such motions would lead to very high and potentially life threatening HIC values in case of impact, c.f. Fig. 2.

In reality the limited elastic deflection $\varphi_{\max}$ is defining the maximum stored potential energy. This leads to a maximum link velocity, which is given by motor maximum velocity plus a term depending on the amount of the stored potential energy

$$\dot{q}_{\max} = \dot{\theta}_{\max} + \Delta\dot{q}_{\max} \tag{16}$$

The velocity increase $\Delta\dot{q}_{\max}$ depends on the maximum motor velocity and the elastic energy.

$$\Delta\dot{q}_{\max} = -\dot{\theta}_{\max} + \sqrt{\dot{\theta}^2_{\max} + \frac{2}{M} E_{\max}(\varphi, \sigma^*)}, \tag{17}$$

with $E_{\max}(\varphi, \sigma^*)$ being the maximum spring energy achievable by means of passive joint deflection. Please note that we assume constant stiffness preset σ^* for simplicity. This means for example that for achieving twice the velocity on the link side, the elastic energy has to be $E_{\max}(\varphi, \sigma^*) = 3\frac{2}{M}\dot{\theta}^2_{\max}$.

The maximum elastic energy for the QA-Joint is therefore

$$E_{\max}(\varphi, \sigma^*) = \int_0^{\varphi_{\max}} \tau_J \mathrm{d}\varphi \tag{18}$$

$$= 40 \int_0^{\varphi_{\max}} e^{15\varphi - \sigma^*} \mathrm{d}\varphi - 40 \int_0^{\varphi_{\max}} e^{-15\varphi - \sigma^*} \mathrm{d}\varphi \tag{19}$$

$$= \frac{8}{3}\left(1 - 2e^{-15\sigma^*} + e^{-30\varphi_{\max}}\right). \tag{20}$$

The corresponding velocity increase is

$$\Delta\dot{q}_{\max} = -\dot{\theta}_{\max} + \sqrt{\dot{\theta}^2_{\max} + \tfrac{2}{M}\tfrac{8}{3}\left(1 - 2e^{-15\sigma^*} + e^{-30\varphi_{\max}}\right)}, \tag{21}$$

which leads to a tip velocity $\dot{x} \in \mathbb{R}$ of

$$\dot{x}_{\max} = l_M \sqrt{\dot{\theta}^2_{\max} + \tfrac{2}{M}\tfrac{8}{3}\left(1 - 2e^{-15\sigma^*} + e^{-30\varphi_{\max}}\right)}. \tag{22}$$

Inserting (22) in (11) leads to the maximum HIC for the QA-Joint. The maximum motor velocity of the QA-Joint is $\dot{\theta}_{\max} = 220$ deg/sec. and we assume a reflected inertia of 3.0 kg (1 kg load and $M = 0.523$ kgm^2). For a high stiffness preset value $\sigma^* = 15$ deg (lowest possible stiffness characteristic) this leads to an increase in achievable link speed of ≈ 1.24, which in turn increases HIC by ≈ 1.6 (HIC $= 38.76$ in the rigid case[2], compared to HIC $= 61.66$ in the flexible case). This impression of a low value results out of the already very high given maximum motor velocity compared to the storable energy of the spring. If we set $\dot{\theta}_{\max} = 80$ deg/sec, we would achieve a velocity increase of 2.1, leading to an HIC increase by 6.37.

To sum up, due to its possibility to store potential energy and use it for achieving higher link speed, a compliant joint is in principle able to reach higher HIC values (of course for non-negligible link inertia) than its stiff counterpart[3]. However, this interpretation of safety level is also only one sided. If peak velocities are required only for a short period of time, intrinsic joint stiffness is an effective way to fulfill this with lighter robot design and not using a larger motor. In general, we suggest to shift the focus of motivation for intrinsic joint compliance from achieving intrinsic safety of the human to utilizing compliance for joint protection and performance improvement. We believe the aspect of safety needs, similar to stiff joints, very careful analysis of the particular design.

After this theoretical analysis on intrinsic impact properties of intrinsically compliant actuators we present some experimental analysis in the following. For this we carried out impact experiments with the QA-Joint and a mechanical setup (the dummy-dummy), which mimics the impact behavior of a human head [28]. This enables us to experimentally evaluate HIC.

E. Head Injury Criterion: experiments

In the following experiment we equipped the QA-Joint with an additional link side mass and let the joint collide with the dummy-dummy. The motor and link inertia are $B = 0.993374$ kgm^2, $M = 0.523808$ kgm^2 and the link length $l_M = 0.5$ m. The joint was commanded to move on a smooth trapezoidal velocity profile and was controlled using the aforementioned state-feedback controller. The measured acceleration was then used to calculate the resulting HIC values.

In Figure 3 the experimental results for impacting the QA-Joint with the dummy-dummy are shown. They support the simulative predictions very well. The calculated HIC values depend only on the link side velocity and not the stiffness preset at all. The "over quadratic" behavior [12] is clearly confirmed and the measured values are indicating very low injury by means of HIC. The impact velocities were ranging

[2]The HIC was evaluated by (11).

[3]Please note that joint compliance does not inherently come at the cost of higher joint weight. It is e.g. possible to make some structural parts compliant without increasing their weight and have the same energy storage effect.

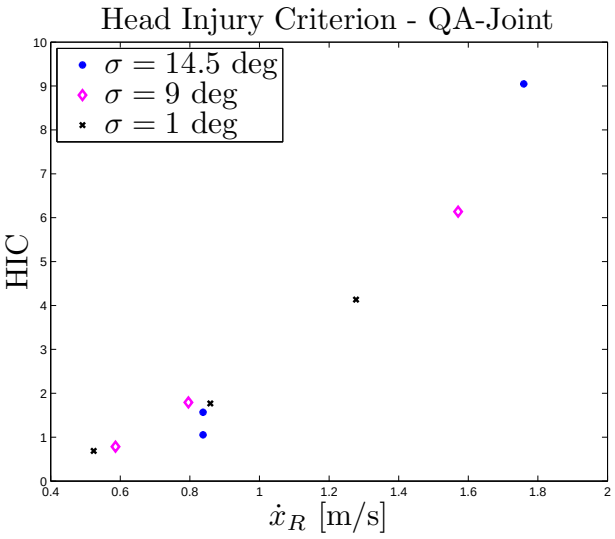

Fig. 3. Head Injury Criterion for the QA-Joint with different impact speeds and stiffness presets.

up to 1.8 m/s, i.e. similar velocities we investigated for various other robots in recent work [23]. The joint shows considerably lower HIC values compared to them, which is mainly due to the lower reflected inertia of the test-joint. Apart from evaluating the injury potential emanating from such a device, we were able to test at the same time the robustness of the proposed control approach from [24]. Although the impact results in large disturbance forces, it was not possible to destabilize the controlled joint.

Apart from the intrinsic properties of collisions, we need sophisticated collision detection and reaction schemes in order to adequately react to external disturbances. This becomes especially important during sharp contact [20].

IV. Collision detection

In this section we introduce two different collision detection methods for intrinsically compliant joints, based only on proprioceptive sensing and certain model knowledge. The first one is the straightforward extension of our work carried out for flexible joint robots.

In order to realize collision detection and reaction schemes based on proprioceptive sensing, it is important to provide an accurate estimation of τ_{ext}. Based on (8)-(10) it is possible to derive two observer structures, which obtain a good estimation of τ_{ext}. The first one utilizes the measured joint torque and the known link side dynamics. The second one relies on motor and link dynamics only and does not require any joint torque sensing.

A. Generalized link side momentum observer

Similar to the collision detection method proposed for a flexible joint robot with joint torque sensing in [29], we can use a momentum based disturbance observer, which uses the measured joint torque and the known rigid body dynamics for collision detection with VIA joints. Instead of a designated joint torque sensor as the strain gauge based ones in the LWR-III, we utilize the motor and link position sensors in combination with the identified torque-deflection characteristics [13], i.e. a model based joint torque sensor. The mathematical derivation is analogous to the one for constant joint elasticity, except for $\tau_J = f(\theta, q, \sigma)$ is a possibly nonlinear relationship as e.g. (10). The result is a first order filtered version of the real external torque denoted as r_1.

B. Generalized joint momentum observer

The following scheme is again based on momentum observation and was already proposed in [30]. We monitor the momentum of both, the motor $p_1 = B\dot{\theta}$ and link inertia $p_2 = M\dot{q}$ and use it for collision detection. Introducing

$$r_2 := K_0 \int \tau_m - g(q) - r_2 \mathrm{d}t - (B\dot{\theta} + M\dot{q}) \tag{23}$$

as the definition for the residual, we can show that

$$r_2 = \frac{K_0}{K_0 + s}\tau_{\text{ext}}. \tag{24}$$

Therefore, we isolated a first-order filtered version of the real external torques with $1/K_0$ being the filter frequency. This signal can be directly used for collision detection and the appropriate reaction, taking into account full information about external forces. The extension to the N-DoF case is straight forward.

Next, the introduced collision detection schemes are analyzed during an abdominal impact with moderate joint stiffness.

C. Collision detection and reaction for the QA-Joint

Figure 4 (left) and Fig. 4 (middle) depict the impact behavior with the abdomen at 100 deg/sec with collision detection activated. As soon as the robot detects the collision, the desired trajectory is stopped abruptly, causing a jump in velocity. The joint stops its motion entirely after ≈ 300 ms.

Figure 4 (right) depicts the real external torque τ_{ext} resulting from impact forces and its estimations r_1, r_2, which are given by the collision detection schemes presented earlier. The cutoff frequency $f_c = 1/K_0$ for both observers is chosen to be 250 Hz. Even though a small lag is therefore present in both cases, the proposed approaches show very quick detection response. r_1 is characterized by some discontinuities in its behavior, which stem from the incorporation of the motor torque saturation in the simulation.

Figure 5 depicts the collision detection and reaction for a position based strategy. Similar to the case of the LWR-III in [29], [31], we use r_i for implementing

$$q_d(t) = -\int K_A\, \hat{r}_i(t)\, \mathrm{d}t + q_{d,c}, \tag{25}$$

where $K_A \in \mathbb{R}^+$ is a gain factor and $q_d, q_{d,c}$ the desired position and the desired position at which the collision occurred. This enables the robot to retract from external collision sources and to show more reactive behavior than simply stopping the robot.

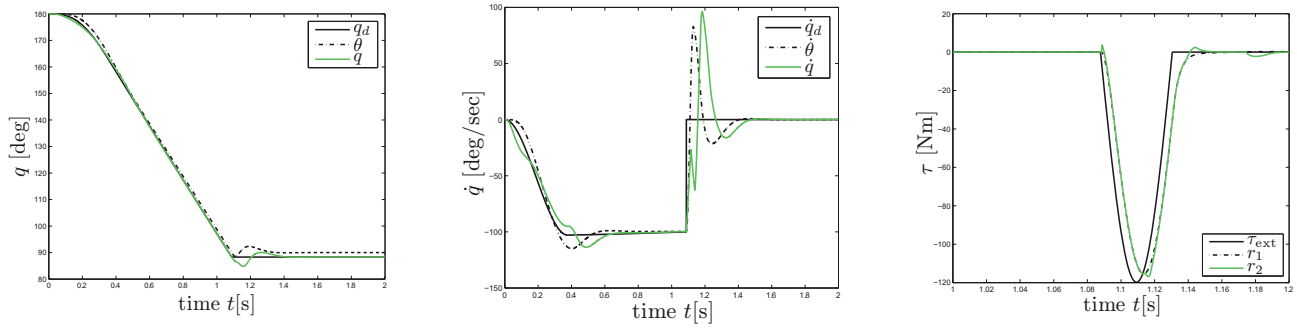

Fig. 4. Desired link position, motor position, and link position for collision detection and reaction (left). Desired link velocity, motor velocity, and link velocity for collision detection and reaction (middle). Real external torque, residual observer 1, and residual observer 2 (right). The reaction strategy is to simply stop the robot.

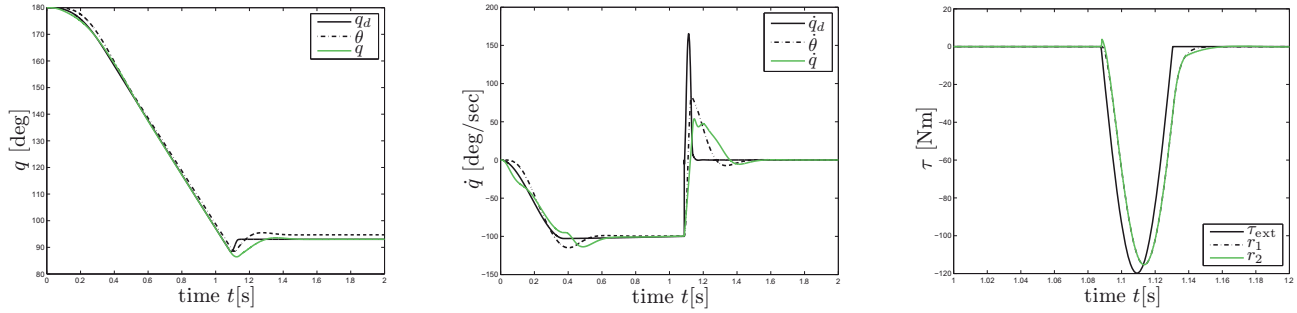

Fig. 5. Desired link position, motor position, and link position for collision detection and reaction (left). Desired link velocity, motor velocity, and link velocity for collision detection and reaction (middle). Real external torque, residual observer 1, and residual observer 2 (right). The reaction strategy is position based.

D. Experimental collision detection performance

Figure 6 depicts the result of the collision detection and reaction experiment. The upper plot visualizes the position of the motor and link side as well as the desired motor position. The lower one depicts the residual and the moment the collision detection activates. In this experiment a simple stop is triggered as soon as an impact is observed. The robot collides at 30 ^{o}/s against the human arm and stops its motion as soon as the threshold 2 Nm for r_1 is exceeded. This value stems mainly from model uncertainties and noise in the order of 1 Nm. Compared to the very high collision speed in the simulations ($\dot{q}_{d,\max} = 100$ deg/s), we chose only $\dot{q}_{d,\max} = 20$ deg/s for the experiments in order to limit the load on the prototype. The sensitivity of our collision detection algorithm for the QA-Joint is comparable to the one for the LWR-III reported in [31]. The accompanying video shows the behavior of the joint with and without collision detection.

V. Conclusion

In this paper we analyzed the role intrinsic joint stiffness plays for safety in physical Human-Robot Interaction. We presented collision detection schemes suited for such devices and analyzed theoretically, as well as experimentally, the possible danger of these new joint designs. Insights concerning the inherently possible velocity increase were elaborated and we discussed this property in the context of intrinsic safety. We showed that the initial motivation for such devices has to be revised when comparing with active compliance approaches. There are two major causes of potential injury, which are related to intrinsic joint stiffness. One of them is dominant for each class of the two designs:

- **Actively compliant robots:** For stiff impacts, motor and link inertia are already decoupled by the moderate joint compliance. However, for lower contact stiffness sophisticated soft-robotics algorithms are needed to ensure compliance by software.
- **Passively compliant robots:** The decoupling of link from motor inertia is always feasible. Nonetheless, it is possible to drive at very high speeds due to intrinsically very low joint stiffness, low damping, and energy storage. In order to tackle that problem, effective vibration damping schemes and the safe limitation of the maximum velocities by software are needed.

Apart from these two major aspects differentiating the inherent joint designs, it is absolutely crucial to develop collision detection schemes with high sensitivity for injury prevention for both joint classes. Clear advantages of intrinsic joint compliance on the other hand are significantly better joint protection during impacts with the environment and the large performance increase that is possible.

To sum up we believe it is important to distinguish two modes for intrinsically compliant joints:

1) **human-friendly mode**
2) **high-performance mode**

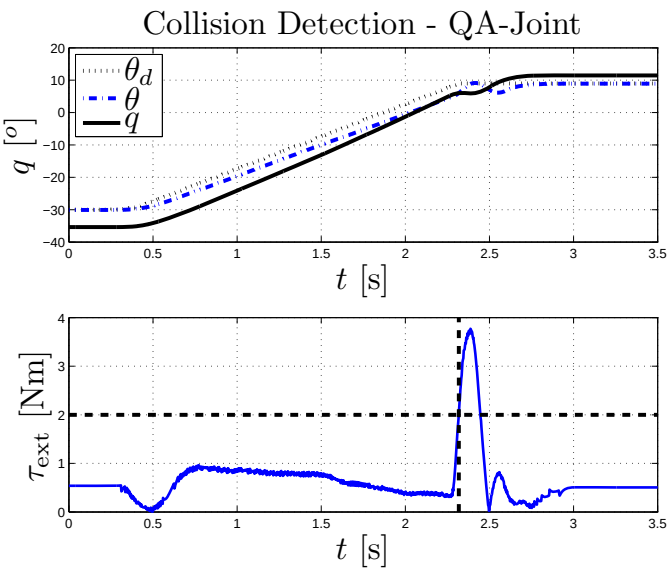

Fig. 6. Collision detection experiment with the QA-Joint.

The **human-friendly mode** focuses on providing intrinsically compliant behavior, while suppressing unwanted oscillations that may easily lead to high and therefore dangerous robot velocities. In order to provide high safety to the human, the stored elastic energy should be supervised, and the full toolbox of methodologies, ranging from collision avoidance, detection, and reaction to higher level fault modules should be embedded in the robot control. The **high-performance mode** on the other hand serves for the full exploitation of energy storage and release for carrying out high-speed motions. This differentiated view makes allowance for the desire of achieving human-like performance while providing safe behavior.

ACKNOWLEDGMENT

This work has been partially funded by the European Commission's Sixth Framework Programme as part of the project VIACTORS under grant no. 231554.

REFERENCES

[1] SMErobot: The European Robot Initiative for Strengthening the Competitiveness of SMEs in Manufacturing, "SMErobot web site," 2007, http://www.smerobot.org/.

[2] PHRIENDS: Physical Human-Robot Interaction: Dependability and Safety, "PHRIENDS web site," 2007, http://www.phriends.eu/.

[3] ROESETTA: Robot control for Skilled Execution of Tasks in natural interaction with humans based on Autonomy, cumulative knowledge and learning, "ROSETTA web site," 2010, http://www.fp7rosetta.org/.

[4] A. Bicchi and G. Tonietti, "Fast and Soft Arm Tactics: Dealing with the Safety-Performance Trade-Off in Robot Arms Design and Control," *IEEE Robotics & Automation Mag.*, vol. 11, pp. 22–33, 2004.

[5] M. Zinn, O. Khatib, and B. Roth, "A New Actuation Approach for Human Friendly Robot Design," *Int. J. of Robotics Research*, vol. 23, pp. 379–398, 2004.

[6] T. Morita, H. Iwata, and S. Sugano, "Development of human symbiotic robot: WENDY," in *IEEE Int. Conf. on Robotics and Automation (ICRA1999), Detroit, USA*, 1999, pp. 3183–3188.

[7] S. A. Migliore, E. A. Brown, and S. P. DeWeerth, "Biologically Inspired Joint Stiffness Control," in *IEEE Int. Conf. on Robotics and Automation (ICRA2005), Barcelona, Spain*, 2005.

[8] G. Palli, C. Melchiorri, T. Wimböck, M. Grebenstein, and G. Hirzinger, "Feedback linearization and simultaneous stiffness-position control of robots with antagonistic actuated joints," in *IEEE Int. Conf. on Robotics and Automation (ICRA2007), Rome, Italy*, 2007, pp. 2928–2933.

[9] B. Vanderborght, B. Verrelst, R. V. Ham, M. V. Damme, D. Lefeber, B. Duran, and P. Beyl, "Exploiting natural dynamics to reduce energy consumption by controlling the compliance of soft actuators," *Int. J. Robotics Research*, vol. 25, no. 4, pp. 343–358, 2006.

[10] S. Wolf and G. Hirzinger, "A new variable stiffness design: Matching requirements of the next robot generation," *IEEE Int. Conf. on Robotics and Automation (ICRA 2008), Pasadena, USA*, pp. 1741–1746, 2008.

[11] S. Haddadin, T. Laue, U. Frese, and G. Hirzinger, "Foul 2050: Thoughts on Physical Interaction in Human-Robot Soccer," in *IEEE/RSJ International Conference on Intelligent Robots and Systems (IROS2007), San Diego, USA*, 2007, pp. 3243–3250.

[12] S. Haddadin, A. Albu-Schäffer, and G. Hirzinger, "Safety Evaluation of Physical Human-Robot Interaction via Crash-Testing," *Robotics: Science and Systems Conference (RSS2007)*, 2007.

[13] O. Eiberger, S. Haddadin, A. Weis, Michael Albu-Schäffer, and G. Hirzinger, "On joint design with intrinsic variable compliance: Derivation of the DLR QA-Joint," *IEEE Int. Conf. on Robotics and Automation (ICRA2008), Anchorage, Alaska*, 2010.

[14] I. P. Herman, *Physics of the Human Body*. Springer Verlag, 2007.

[15] S. Haddadin, T. Laue, U. Frese, S. Wolf, A. Albu-Schäffer, and G. Hirzinger, "Kick it like a safe robot: Requirements for 2050," *Robotics and Autonomous Systems: Special Issue on Humanoid Soccer Robots*, vol. 57, pp. 761–775, 2008.

[16] A. Edsinger, "Robot manipulation in human environments," Ph.D. dissertation, Massachusetts Institute of Technology, Department of Electrical Engineering and Computer Science, 2007.

[17] J.-J. Park, H.-S. Kim, and J.-B. Song, "Safe robot arm with safe joint mechanism using nonlinear spring system for collision safety," *IEEE Int. Conf. on Robotics and Automation (ICRA2009), Kobe, Japan*, pp. 3371–3376, 2009.

[18] A. Albu-SchÄffer, O. Eiberger, M. Grebenstein, S. Haddadin, C. Ott, T. WimbÖck, S. Wolf, and G. Hirzinger, "Soft robotics: From torque feedback controlled lightweight robots to intrinsically compliant systems," *Ieee Robotics And Automation Magazine*, vol. 15, no. 3, pp. 20 – 30, 2008.

[19] S. Haddadin, A. Albu-Schäffer, and G. Hirzinger, "Safe Physical Human-Robot Interaction: Measurements, Analysis & New Insights," in *International Symposium on Robotics Research (ISRR2007), Hiroshima, Japan*, 2007, pp. 439–450.

[20] ——, "Soft-tissue injury in robotics," *IEEE Int. Conf. on Robotics and Automation (ICRA2010), Anchorage, Alaska*, 2010.

[21] M. Wassink and S. Stramigioli, "Towards a Novel Safety Norm for Domestic Robots," in *IEEE/RSJ Int. Conf. on Intelligent Robots and Systems (IROS2007), San Diego, USA*, 2007.

[22] B. Povse, D. Koritnik, R. Kamnik, T. Bajd, and M. Munih, "Cooperation of human operator and small industrial robot," *Int. Journal of Automation Austria*, vol. 18, no. 1, pp. 80–86, 2010.

[23] S. Haddadin, A. Albu-Schäffer, and G. Hirzinger, "Requirements for safe robots: Measurements, analysis & new insights," *Int. J. of Robotics Research*, 2009.

[24] A. Albu-Schäffer, S. Wolf, O. Eiberger, S. Haddadin, F. Petit, and M. Chalon, "Dynamic modeling and control of variable stiffness actuators," in *IEEE Int. Conf. on Robotics and Automation (ICRA 2010), Anchorage, Alaska*, 2010.

[25] S. Haddadin, "Evaluation Criteria and Control Structures for safe Human-Robot Interaction," Master's thesis, Technical University of Munich & German Aerospace Center (DLR), 12 2005.

[26] S. Oberer and R. D. Schraft, "Robot-Dummy Crash Tests for Robot Safety Assessment," in *IEEE Int. Conf. on Robotics and Automation (ICRA2007), Rome, Italy*, 2007, pp. 2934–2939.

[27] D. Gao and C. W. Wampler, "On the use of the head injury criterion (hic) to assess the danger of robot impacts," *IEEE Robotics and Automation Magazine*, 2009.

[28] S. Haddadin, A. Albu-Schäffer, and G. Hirzinger, "The Role of the Robot Mass and Velocity in Physical Human-Robot Interaction - Part I: Unconstrained Blunt Impacts," in *IEEE Int. Conf. on Robotics and Automation (ICRA2008), Pasadena, USA*, 2008, pp. 1331–1338.

[29] A. De Luca, A. Albu-Schäffer, S. Haddadin, and G. Hirzinger, "Collision detection and safe reaction with the DLR-III lightweight manipulator arm," *IEEE/RSJ Int. Conf. on Intelligent Robots and Systems (IROS2006), Beijing, China*, pp. 1623–1630, 2006.

[30] A. D. Luca, F. Flacco, R. Schiavi, and A. Bicchi, "Nonlinear decoupled motion-stiffness control and collision detection/reaction for the vsa-ii

variable stiffness device," *IEEE/RSJ Int. Conf. on Intelligent Robots and Systems (IROS2010), St.Louis, USA*, pp. 5487–5494, 2009.

[31] S. Haddadin, A. Albu-Schäffer, A. De Luca, and G. Hirzinger, "Collision Detection & Reaction: A Contribution to Safe Physical Human-Robot Interaction," in *IEEE/RSJ Int. Conf. on Intelligent Robots and Systems (IROS2008), Nice, France*, 2008.